



**HAL**  
open science

## Dynamics of the energy transfer involved in a diarylethene-perylenebisimide dyad: comparison between the molecule and the nanoparticle level

Nicolas Fabre, Tuyoshi Fukaminato, Arnaud Brosseau, Michel Sliwa, Rémi Métivier

### ► To cite this version:

Nicolas Fabre, Tuyoshi Fukaminato, Arnaud Brosseau, Michel Sliwa, Rémi Métivier. Dynamics of the energy transfer involved in a diarylethene-perylenebisimide dyad: comparison between the molecule and the nanoparticle level. *Photochemical & Photobiological Sciences*, 2023, 22 (7), pp.1673-1681. 10.1007/s43630-023-00405-5 . hal-04404382

**HAL Id: hal-04404382**

**<https://hal.science/hal-04404382>**

Submitted on 18 Jan 2024

**HAL** is a multi-disciplinary open access archive for the deposit and dissemination of scientific research documents, whether they are published or not. The documents may come from teaching and research institutions in France or abroad, or from public or private research centers.

L'archive ouverte pluridisciplinaire **HAL**, est destinée au dépôt et à la diffusion de documents scientifiques de niveau recherche, publiés ou non, émanant des établissements d'enseignement et de recherche français ou étrangers, des laboratoires publics ou privés.



Distributed under a Creative Commons Attribution 4.0 International License

# Dynamics of the energy transfer involved in a diarylethene-perylenebisimide dyad: comparison between the molecule and the nanoparticle level

Nicolas Fabre,<sup>a</sup> Tuyoshi Fukaminato,<sup>b,\*</sup> Arnaud Brosseau,<sup>a</sup> Michel Sliwa,<sup>c,\*</sup> Rémi Métivier<sup>a,\*</sup>

<sup>a</sup> *Université Paris-Saclay, ENS Paris-Saclay, CNRS, PPSM, 91190 Gif-sur-Yvette, France*

<sup>b</sup> *Kumamoto University, Department of Applied Chemistry & Biochemistry, Kumamoto 860-8555, Japan*

<sup>c</sup> *Univ. Lille, CNRS, UMR 8516, LASIRE, Laboratoire de Spectroscopie pour les Interactions, la Réactivité et l'Environnement, F59 000, Lille, France*

\* *Corresponding authors.*

E-mail addresses: tuyoshi@kumamoto-u.ac.jp (T. Fukaminato), michel.sliwa@univ-lille.fr (M. Sliwa), remi.metivier@ens-paris-saclay.fr (R. Métivier)

Keywords: Photochromism; Fluorescence; FRET; Photodynamics; Diarylethene; Perylenebisimide

## Abstract

Photochromic materials are widely used to achieve fluorescence photoswitching. Understanding the energy transfer processes occurring in these systems would be an advantage for their use and a better optimization of their properties. In this scope, we studied a diarylethene-perylenebisimide (**DAE-PBI**) dyad that presents a bright red emission and a large ON-OFF contrast, both in solution and in an aqueous suspension of nanoparticles (NPs). Using ultrafast transient absorption spectroscopy, the excited state dynamics was characterized for this dyad in THF solution and compared to its behavior in NPs state. An efficient energy transfer process between the PBI fluorophore and the DAE photochromic unit in its closed form was demonstrated, occurring in a few hundreds of femtoseconds.

## Introduction

Fluorescent photochromic materials are emerging systems due to their promising applications in several fields such as bioimaging or super-resolution microscopy.<sup>1-4</sup> A common way to prepare these fluorescent switches is the combination of photochromic and fluorescent moieties within a molecular dyad.<sup>5,6</sup> Among the photochromic molecules, diarylethenes (DAE) have attracted particular attention because of their excellent bistability, conversion yield and fatigue resistance.<sup>7</sup> When a DAE unit is combined to a suitable fluorophore through a non-conjugated spacer, the fluorescence can be modulated by means of a Förster resonance energy transfer (FRET).<sup>8</sup> In the case of DAE-based dyads, the open form (OF) is emissive whereas the closed form (CF) is not: the DAE-CF isomer has an absorption band overlapping the emission band of the fluorophore, thus playing the role of energy acceptor.<sup>9</sup> Following this concept, a large number of molecular systems based on controllable fluorescence photoswitching have been described.<sup>5,6,10-12</sup> Recently, we have reported a molecular dyad composed of a DAE (photochromic part) and a perylenebisimide (PBI, fluorescent part), showing appealing properties.<sup>13</sup> The emission is over 600 nm and the energy transfer from the PBI to the DAE-CF is very efficient, estimated to reach almost unity. Moreover, when the dyads are gathered into nanoparticles (NPs), intermolecular energy transfer processes are favored, enhancing substantially the photoswitching properties. To better understand, characterize and compare these energy transfer processes in both solution and suspension of NPs, probing the dynamics of the excited state by transient absorption spectroscopy is a method of choice.<sup>14-16</sup> As PBI and DAE are well-known molecules, their respective dynamics are often described in the literature.<sup>7,17,18</sup> However, it should be stressed here that ultrafast dynamics studies of organic nanoparticles are scarce in the literature due to their intrinsic heterogeneity and existence of multi-excitonic processes.<sup>16,19</sup> Herein, we focus on the **DAE-PBI** dyad (Figure 1) to unravel the ultrafast processes, especially FRET, occurring between the PBI donor and the DAE-CF acceptor. We propose a de-excitation pathway for the solution state, and we highlight the differences between the solution and the NPs state.

## Results and discussion

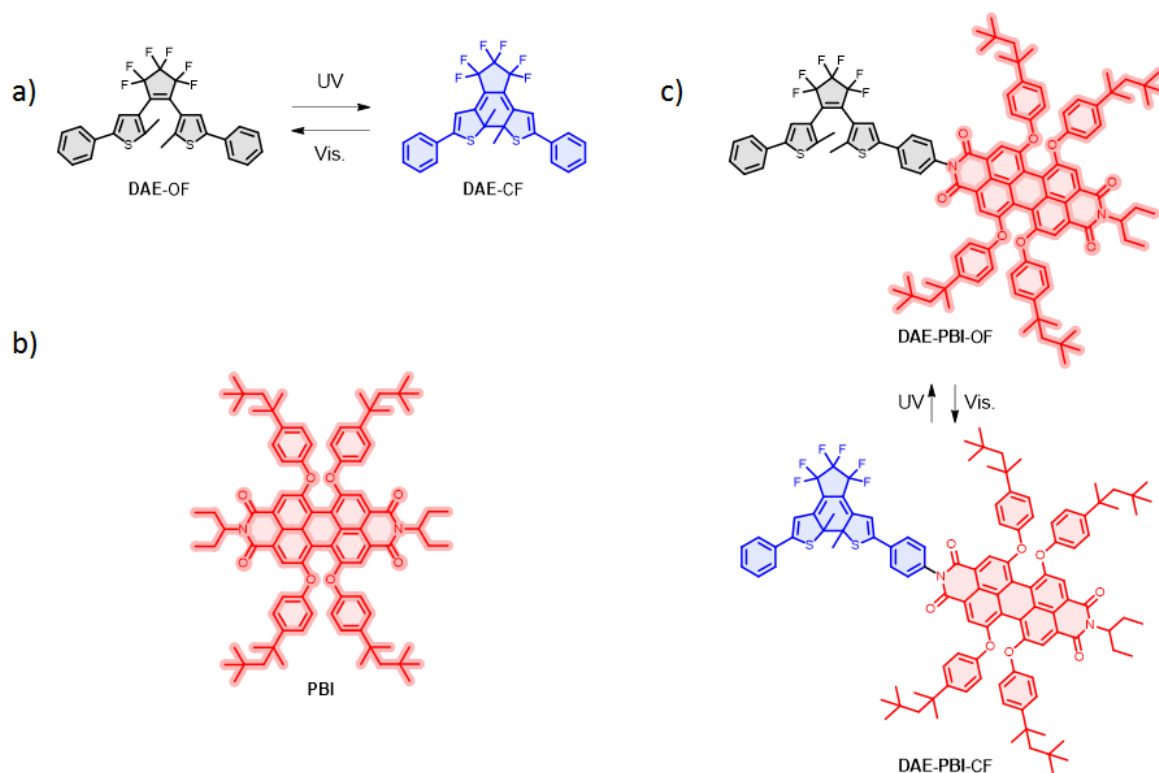


Figure 1. Molecular structures of the **DAE** photochromic model compound, the **PBI** model fluorophore, and the **DAE-PBI** dyad derivative (OF: open form, CF: closed form).

The **DAE** photochromic model molecule, the **PBI** model fluorophore, and the **DAE-PBI** dyad were synthesized via previously reported procedures<sup>13</sup> and displayed in Figure 1. Absorption and emission spectra of the three molecules are shown in Figure 2, both in solution (THF) and as a suspension of NPs in water, prepared by the reprecipitation method as mentioned in the Supporting Information (SI). The average diameter of the NPs was determined by Dynamic Light Scattering (DLS) to be  $110 \pm 30$  nm (see SI). Concerning the **DAE-PBI** dyad in the OF, the absorption spectra are similar in THF solution and in NPs. The two absorption bands at 400-450 nm and 475-610 nm are related to the  $S_0 \rightarrow S_2$  and  $S_0 \rightarrow S_1$  electronic transitions of the PBI moiety. In the UV range, the observed band around 300 nm is an overlay of both the DAE-OF and PBI units. Under UV irradiation at 365 nm, in solution and in the NPs state, a photostationary state (PSS-365) is reached, corresponding to a mixture of 85% DAE-CF and 15% DAE-OF isomers: a band from 600 to 700 nm arises due to the photogenerated CF of the DAE part, as well

as the appearance of a band at 350-400 nm and a decrease of the band at 300 nm. Concerning the emission spectra, the OF dyad is fluorescent with an emission spectrum similar to the one of the **PBI** model fluorophore in the related state, in the range 580-750 nm in solution and 600-800 nm in NPs. The fluorescence quantum yield ( $\Phi_{\text{fluo}}$ ) is estimated for **DAE-PBI-OF** at  $0.91 \pm 0.09$  in solution but  $0.09 \pm 0.01$  in NPs. Similar values of  $\Phi_{\text{fluo}}$  were found for the **PBI** model fluorophore, i.e.  $0.93 \pm 0.07$  in solution and  $0.09 \pm 0.01$  in NPs. This difference of emission quantum yields between solution and NPs can be rationalized by the existence of quenching processes due to intermolecular interactions. Another important difference between THF solution and NPs suspension is observed at the PSS-365, for which a fluorescence signal remains in solution (Figure 2c, due to the residual DAE-OF molecules) whereas it is completely quenched (Figure 2f,  $\Phi_{\text{fluo}} \approx 0$ ) in the NPs state.

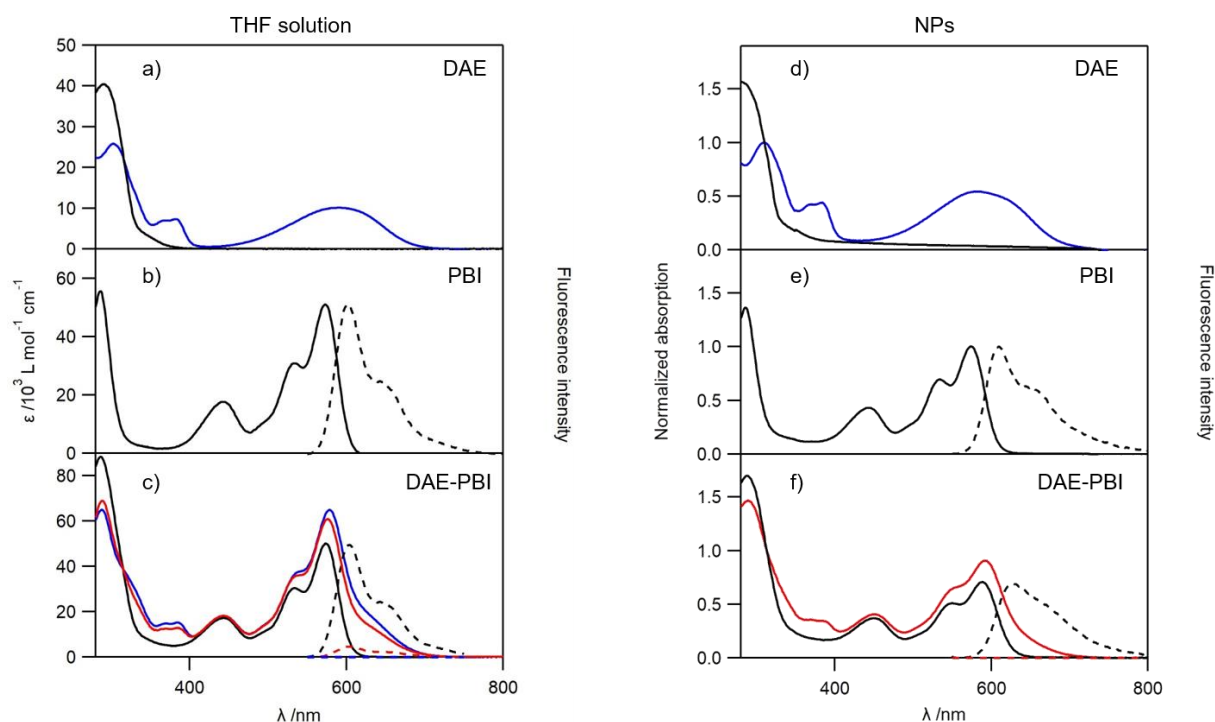


Figure 2. Absorption (full line) and emission spectra (dotted line,  $\lambda_{\text{exc}} = 540$  nm) in THF solution for **DAE** (a), **PBI** (b), **DAE-PBI** (c) and in a water suspension of NPs for **DAE** (d), **PBI** (e) and **DAE-PBI** (f) in OF (black), CF (blue) and PSS-365 (red).

Fluorescence decays in THF solution are plotted in Figure 3a and fluorescence lifetimes of **PBI** and **DAE-PBI** were determined at  $6.51 \pm 0.04$  ns and  $6.00 \pm 0.04$  ns respectively by means of the time-correlated single photon counting (TCSPC) technique. At the PSS-365, the fluorescence is totally quenched in NPs, preventing any decay measurement. However, as the **DAE-PBI** dyad is still emissive at PSS-365 in THF solution, fluorescence lifetime can be determined, and remains at  $6.00 \pm 0.04$  ns,

supporting the presence of extremely efficient energy transfer process. Indeed, such energy transfer from the PBI to the DAE-CF unit, corresponding to very short decay-time (expected to be  $< 0.4$  ps according to the Förster theory), and a very limited number of photons, is too fast to be recorded by our TCSPC instrument (instrumental response function IRF  $\sim 23$  ps full width at half maximum, FWHM), the remaining dyads in the **DAE-PBI-OF** being responsible for the observed fluorescence. In the NPs state, the fluorescence decays are no longer mono-exponential, as it is observed on Figure 3b. For NPs of **PBI**, four fluorescence decay times are determined at  $4.97 \pm 0.04$  ns,  $2.31 \pm 0.04$  ns,  $0.44 \pm 0.03$  ns and  $0.04 \pm 0.03$  ns and are in agreement with the literature.<sup>20</sup> The existence of sub nanosecond components (about 85%) are in line with the low fluorescence quantum yield. This shortening of the decay time constants can be explained by different intermolecular interactions and microenvironments of **PBI** in the NPs compared to the solvated molecules in THF, such as aggregates or excimer species leading to some “molecular traps” that increase relaxation probability.<sup>21</sup> Therefore, a distribution of decay times is observed and represent the probability of the exciton to relax in the different energy traps. Concerning the **DAE-PBI-OF** dyad, three fluorescence time constants are determined in the NPs state at  $5.03 \pm 0.04$  ns,  $0.57 \pm 0.03$  ns and  $0.05 \pm 0.03$  ns in agreement with a fluorescence quantum yield of 0.09. All the fluorescence lifetimes are gathered in Table 1.

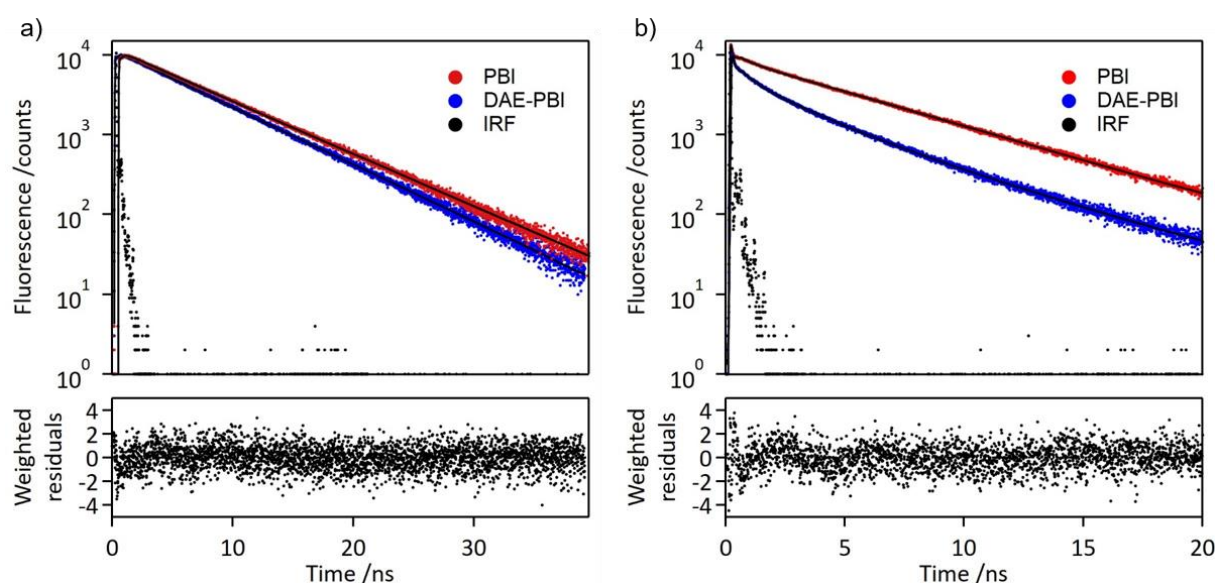


Figure 3. Fluorescence decays for **PBI** (red dots) and **DAE-PBI-OF** (blue dots) in a) THF solution and b) water suspension of NPs, measured at  $\lambda_{exc} = 490$  nm and  $\lambda_{obs} = 600$  nm, curve fitting (black line), and instrumental response function (IRF, black dots).

	$\tau_1$ / ns (a <sub>1</sub> , f <sub>1</sub> )	$\tau_2$ / ns (a <sub>2</sub> , f <sub>2</sub> )	$\tau_3$ / ns (a <sub>3</sub> , f <sub>3</sub> )	$\tau_4$ / ns (a <sub>4</sub> , f <sub>4</sub> )	$\Phi_{\text{fluo}}$
<b>PDI</b> (THF)	6.51±0.04 (1.00, 1.00)	–	–	–	0.93
<b>DAE-PDI-OF</b> (THF)	6.00±0.04 (1.00, 1.00)	–	–	–	0.91
<b>PDI</b> (NPs)	4.97±0.04 (0.03, 0.31)	2.31±0.04 (0.11, 0.52)	0.44±0.03 (0.12, 0.11)	0.04±0.03 (0.74, 0.06)	0.09
<b>DAE-PDI-OF</b> (NPs)	5.03±0.04 (0.37, 0.97)	0.57±0.03 (0.03, 0.01)	0.05±0.03 (0.60, 0.02)	–	0.09

Table 1. Decay time constants ( $\lambda_{\text{exc}} = 490$  nm), normalized pre-exponential factors and fractions of intensity obtained at  $\lambda_{\text{em}} = 600$  nm after global analysis at five emission wavelengths (600, 620, 640, 660, 680 and 700 nm), and emission quantum yields ( $\pm 10\%$  accuracy) for **PBI** and **DAE-PBI-OF**, in THF solution and in the NPs state.

To have access to the energy transfer rate between the DAE and PBI moieties within the **DAE-PBI** dyad, transient femtosecond absorption measurements were carried out, first on the two model compounds (**PBI**, **DAE**) and then on the dyad. For the **PBI** in THF solution upon 435 nm excitation, after an ultrafast internal conversion of S<sub>2</sub> to S<sub>1</sub> (time constant about 120 fs), a characteristic time constant of 4.6 ps is found for the relaxation of the hot S<sub>1</sub> formed (bathochromic shift of the extremum of the negative band) before the long-lived emissive cold state S<sub>1</sub>, finally decaying with a lifetime of 6.5 ns (Figure SI-1 and SI-2). Concerning the **DAE-CF** excited at 570 nm, the evolution of transient spectra is described by three time-constants: the conversion of the 1B state to 2A state occurs in 440 fs, then the 2A state relaxes in 1.9 ps followed by the internal conversion to the ground state through the conical intersection in 8 ps with 3% of cycloreversion (Figure SI-3 and SI-4). The dynamics of the excited state of molecules similar to those of **PBI** and **DAE-CF** model compounds have been already reported in close experimental conditions and are in agreement with our results.<sup>17,18</sup> The evolution of transient absorption spectra and decay associated spectra (DAS) corresponding to the two compounds are shown in the Supporting Information (Figure SI-1 to SI-4).

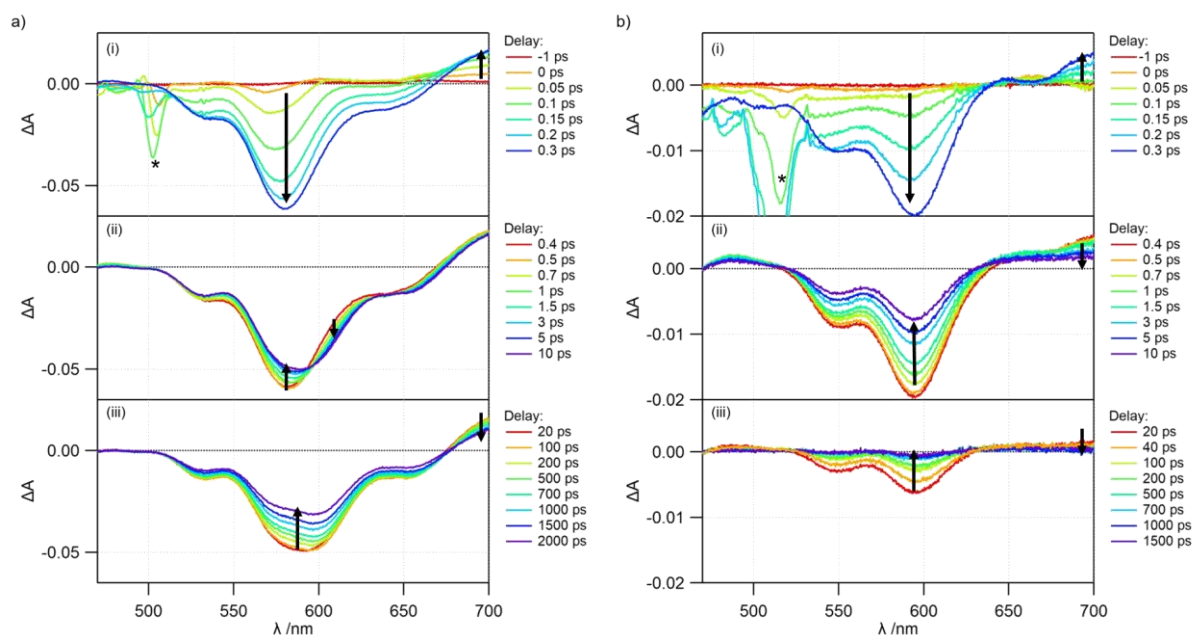


Figure 4. Femtosecond transient difference absorption spectra for **DAE-PBI-OF** in a) THF solution and b) NPs at different pump-to-probe time-intervals (pump beam at 435 nm with an energy of 1.15  $\mu\text{J}$  per pulse). The three frames show the evolution of the spectra over different time ranges: (i) -1 fs to 300 fs, (ii) 400 fs to 10 ps and (iii) 20 ps to 2000 ps. Stimulated Raman amplification signals from the solvent (\*) are observed between 500 and 520 nm at time delays shorter than 300 fs.

To investigate the dynamics of the excited states of **DAE-PBI**, especially the energy transfer process between the PBI fluorophore and the DAE moiety, experiments were first conducted on the **DAE-PBI-OF** dyad in THF solution. The evolution of difference absorption spectra under excitation at 435 nm are displayed Figure 4a. The DAE moiety does not absorb at 435 nm, therefore only the PBI molecular fragment is excited. The measured spectra are comparable to those obtained for the **PBI** molecule (Supporting Information, Figure SI-1). Within the excitation pulse (instrumental response function 110 fs FWHM), the difference absorption spectra grow from 0 to 300 fs time delay. During this time, the rising of the Franck Condon  $S_2$  excited state and its ultrafast internal conversion to  $S_1$  occur (Figure 4a-i). At 300 fs, the transient spectrum is characterized by a broad negative band corresponding to the depopulation of the ground state and the stimulated emission of excited states, which extends from 500 to 670 nm, and a positive band corresponding to the absorption of the hot excited state  $S_1$  ( $> 650$  nm). A bathochromic shift of the extremum of the negative band is observed within 2 ps (from 580 nm to 590-600 nm, Figure 4a-ii), as it was also observed for the model **PBI** (Figure SI-1), can be attributable to the

vibrational relaxation of the hot  $S_1$ . Beyond 20 ps, all bands fade simultaneously (Figure 4a-iii). As for **PBI**, the de-excitation process to the ground state is not complete after 2000 ps, which is in accordance with the fluorescence lifetime of the **DAE-PBI** dyad, estimated to be  $6.00 \pm 0.04$  ns by TCSPC in solution. A numerical fitting is performed globally, using a sum of two exponentials convoluted with a Gaussian pulse of 110 fs (FWHM) and an offset for the long-lived emissive relaxed  $S_1$  state (6.00 ns) that provides characteristic time constants of 120 fs and 5.4 ps, corresponding respectively to the rising of the signal mixed with internal conversion (convoluted by instrumental response function) and vibrational relaxation of the hot  $S_1$  state (Supporting Information, Figure SI-5). These relaxation decay-times are comparable to the ones determined for the **PBI** model compound.

Concerning the NPs state, the transient absorption spectra for **PBI** and **DAE-PBI-OF** upon 435 nm excitation are displayed in Figure SI-6 and Figure 4b, respectively. Transient spectra and time constants are comparable, as expected from their similar fluorescence quantum yields and lifetimes (Table 1). As for the THF solution, the broad negative band of **DAE-PBI-OF** NPs related to the depopulation of ground state and stimulated emission of excited states is observed, as well as the positive one corresponding to the  $S_1$  absorption. However, after 2000 ps, the excited states of the dyads relax entirely. In agreement with the time-resolved fluorescence analysis (Table 1), the decay is multiexponential with almost 70% recovery in few tens of picoseconds (see depopulation recovery, comparing the transient spectra at 10 ps vs. 0.4 ps in Figure 4b-ii). A global numerical fitting using four exponentials convoluted with a Gaussian pulse of 110 fs (FWHM) and an offset for the long-lived emission (averaged fluorescence decay times  $> 100$  ps determined by single photon counting, weighted by their pre-exponential coefficients) provides four characteristic times for **DAE-PBI-OF** and **PBI** in the NPs state, at 110 fs (rising component), 190 fs, 2.8 ps, 52.3 ps and 70 fs (rising component), 310 fs, 2.6 ps, 41.3 ps, respectively. The first characteristic time constant around 100 fs is attributed to the internal conversion to hot  $S_1$  of the PBI moiety (Supporting Information, Figure SI-7 and SI-8). The three other characteristic times, few hundreds of femtoseconds, few picoseconds and few tens of picoseconds are related to nonradiative deactivation paths from the  $S_1$  state to the ground state, the few tens of picosecond time constant being consistent with the short decay time-constant determined by TCSPC (0.04 ns and 0.05 ns,

*vide supra*). The kinetics of femtosecond transient spectra showed that, compared to PBI in solution, there are two extra short decays that rationalized the low fluorescence quantum yield in NPs. As pointed above, these decays could be assigned to the existence of different PBI trap species (dark aggregates), however contribution from multi-exciton processes such as singlet-singlet annihilation cannot be discarded and will be studied in the future (see Supporting Information for a detailed calculation of the average number of molecules excited per NP during one laser pulse).<sup>22</sup> Indeed, such processes could lead to enhanced redox properties of PBI moieties in the excited state<sup>23</sup> as well as improved photoreactivity of photochromic derivatives<sup>24</sup> especially in the case of DAE.<sup>25</sup> The next step is to characterize the energy transfer characteristic time constant taking place between the PBI fluorophores and the DAE moieties in the CF, therefore experiments at the PSS-365 are required.

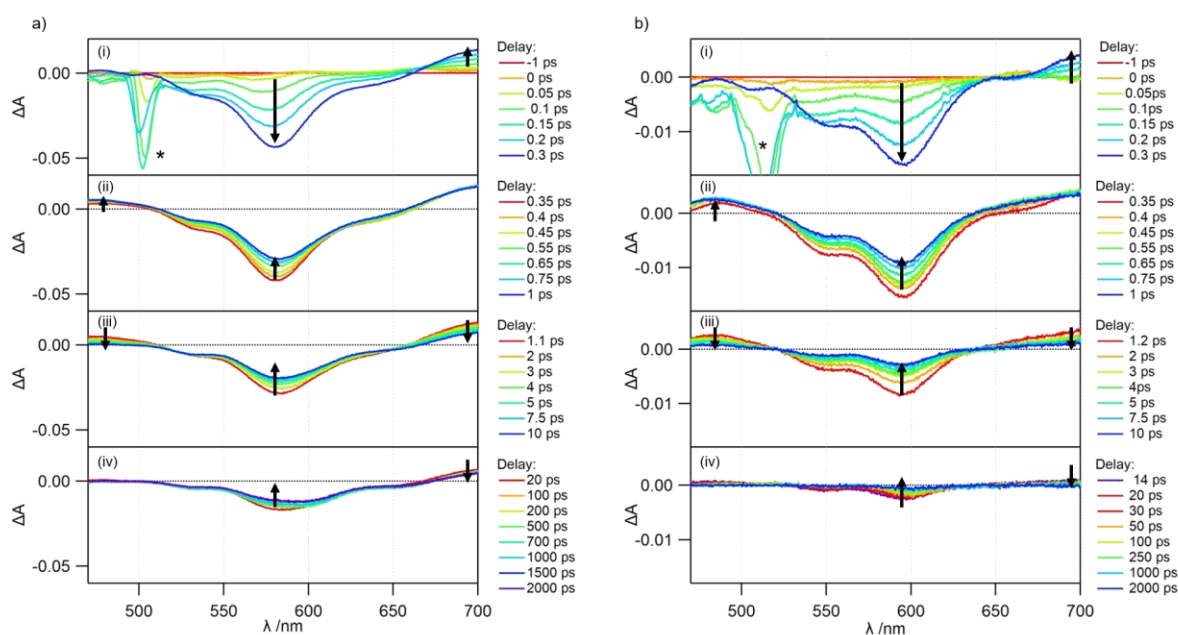


**Figure 5.** Femtosecond transient difference absorption spectra for **DAE-PBI** at the PSS-365 in a) THF solution and b) the NPs state at different pump-to-probe time-intervals (pump beam at 435 nm with an energy of 1.15  $\mu$ J per pulse). The four frames show the evolution of the spectra over different time ranges: (i) -1 fs to 300 fs, (ii) 350 fs to 1 ps, (iii) 1.1 ps to 10 ps and (iv) 14 ps to 2000 ps. Stimulated Raman amplification signals from the solvent (\*) are observed between 500 and 520 nm at time delays shorter than 300 fs.

The difference absorption spectra for the **DAE-PBI** dyad at PSS-365 in THF solution under excitation at 435 nm are displayed in Figure 5a. As mentioned previously, the PSS-365 is a mixture of 15% **DAE-PBI-OF** and 85% **DAE-PBI-CF**. Both absorb light and contribute to the observed dynamics. As for the dyad in OF, the CF of the DAE part does not absorb at 435 nm, only the PBI is excited by the pump laser beam. Thus, right after excitation, at 300 fs time delay, the transient spectra are characteristic of the  $S_1$  hot state of the PBI fluorophore. As for **DAE-PBI-OF**, we observe the negative band attributable to the ground state depopulation and the stimulated emission of excited states (500-670 nm), as well as the positive bands corresponding to the excited states absorption ( $> 670$  nm). However, over the 400 fs - 1.5 ps time range, while for **DAE-PBI-OF** a band shift was observed for the vibrational relaxation of the hot  $S_1$ , the evolution of the signals is different for **DAE-PBI-CF**. A one-third decrease in the negative band is observed during this time interval, while the positive band extending beyond 670 nm increases and a positive band at 470 nm appears. These features are clearly assigned to the formation of the excited DAE-CF. The DAE-CF thus becomes excited over a time interval corresponding to the rapid depopulation band decrease centered at 570 nm, characteristic of the PBI fragment. This concomitant deactivation of the PBI excited state and appearance of the excited DAE-CF is a clear signature of the energy transfer process occurring from the PBI (donor) to the DAE-CF (acceptor). The evolution after 1.5 ps is an overlay of the dynamics of (i) PBI excited in **DAE-PBI-OF** and (ii) DAE-CF excited after FRET in **DAE-PBI-CF**. DAE-CF dynamics is finished after few tens of picoseconds, therefore beyond 20 ps, the transient difference spectra correspond solely to PBI excited in **DAE-PBI-OF**. As for **PBI** and **DAE-PBI-OF**, the de-excitation process is not complete after 2000 ps since the lifetime of the  $S_1$  excited state of the PBI unit is 6.0 ns.

Four exponentials were required to describe the evolution of the transient spectra, determined at 70 fs, 210 fs, 3.5 ps and 25.4 ps and the DAS are shown in Figure SI-9. The 210 fs DAS is assigned to the FRET process, indeed a decay of stimulated emission and ground state depopulation band of the PBI excited state, concomitant with the formation of the 470 nm band of the DAE-CF excited state. Moreover, the negative part from 630 to 700 nm confirms the formation of the 2A state of DAE-CF whose absorption band is located in this wavelength range. These observations combined to our results

describe above, underline that the 210 fs component is characteristic of FRET from PBI to DAE-CF and internal conversion of 1B to 2A of the DAE-CF, while the 3.5 ps time-constant involves the vibrational relaxation of the hot  $S_1$  state of PBI and the DAE-CF relaxation from its 2A state.

Finally, the longest time of 25 ps is attributed to the de-excitation of the 2A state of the DAE by crossing the potential energy barrier and passing to the ground state via a conical intersection and some relaxation from the hot ground state. The DAS corresponding to these two characteristic times show the same profile as those obtained for the **DAE-CF** model compound (see Figure SI-9) and confirm their assignment to the relaxation dynamics of DAE-CF.

Finally, Figure 6 presents the mechanistic scheme of the **DAE-PBI** dyad in THF solution at the PSS-365. For dyads that are in the CF, after excitation at 435 nm, the PBI fluorophore is promoted to the  $S_2$  state. This is followed by an internal conversion to the  $S_1$  state of PBI, then a relaxation of the hot  $S_1$  state and a resonant energy transfer, leading to the 1B excited state of the DAE-CF which relaxes to the 2A excited state. These steps all proceed within the same time-interval, corresponding to the characteristic time of 210 fs. In the following steps, the excited 2A state of DAE-CF evolves towards the relaxed 2A state in 3.5 ps which can then overcome the potential energy barrier to reach the conical intersection and the ground state in 25.4 ps. Regarding the remaining **DAE-PBI** dyads in the OF, the same de-excitation scheme as the one presented in Supporting Information (Figure SI-5) remains valid.

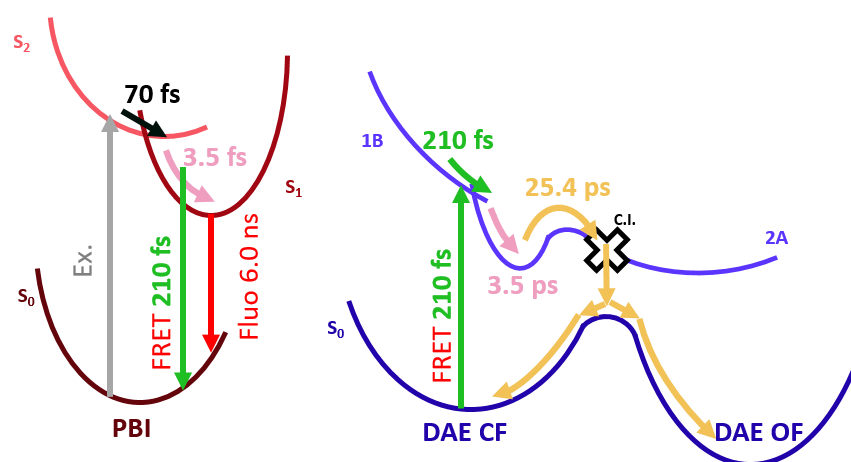


Figure 6. Proposed mechanism for the de-excitation of **DAE-PBI** at the PSS-365 in THF solution after excitation at 435 nm. The conical intersection is represented by a cross.

Considering the NPs state, the differential absorption spectra of the **DAE-PBI** dyad at PSS-365 are displayed in Figure 5b. On the time range from 0 to 0.3 ps, the negative band attributable to the depopulation of the ground state and the stimulated emission of excited states appears (500-650 nm), as well as the positive band corresponding to the absorption of excited states ( $> 670$  nm). As for the dyad at the PSS-365 in THF solution, on the time range from 0.4 to 1 ps, a positive band appears in the 470-500 nm region while the other bands fade. Moreover, after 1 ps all the bands decay simultaneously. Kinetics curve fitting were carried out using four exponentials convoluted with a Gaussian pulse of 110 fs (FWHM) and an offset for the long-lived emission (4.7 ns average of the two long fluorescence decay times determined previously, weighted by their pre-exponential coefficients) providing characteristic times of 80 fs, 135 fs, 1.1 ps and 11.4 ps. The 135 fs DAS are similar to the one observed for **DAE-PBI-CF**, *i.e.* within this time constant FRET occurs with the formation of the excited DAE-CF band. However, it is difficult to determine precisely the FRET time constant and analyze the different DAS since the transient spectra evolution is mixed, with a multiexponential decay as for **DAE-PBI-OF** NPs (Supporting Information, Figure SI-10).

However, a simple comparison between difference absorption spectra of the **DAE-PBI** dyad at PSS-365 in THF solution and NPs state is possible. First, we can notice that the depopulation band decays much faster in NPs than in solution (decrease of  $\Delta A$  by 80% in 10 ps in NPs, compared to 50% in 10 ps in solution), the stimulated emission totally disappears in NPs, and after 1 ns no more excited species can be observed in NPs. All these observations underline that in addition to intramolecular FRET, additional intermolecular relaxation processes can exist in NPs, such as multi-excitonic processes and energy transfer to traps.

In brief, the spectroscopic investigation of **DAE**, **PBI** and **DAE-PBI** compounds in solution has allowed us to highlight that the FRET-type energy transfer from PBI to DAE-CF within the **DAE-PBI-CF** dyad takes place with a time-constant of ca. 210 fs in THF solution. It is possible to compare this experimental value with that calculated applying the Förster theory, given a Förster radius of  $R_0 = 71 \text{ \AA}$ , as it was reported in our previous study.<sup>13</sup> The energy transfer rate-constant estimated at  $k_{ET} = 2.38 \times 10^{12} \text{ s}^{-1}$  provides a characteristic energy transfer time of 420 fs. These two values are rather consistent with each

other. Moreover, we did not observe any characteristic band of cationic species (sharp signals located between 300 and 400 nm) or anionic species, supporting the hypothesis of an absence of photoinduced electron transfer in the **DAE-PBI** dyad.

## Conclusion

In this work, photochromic and fluorescence properties of the **DAE-PBI** dyad were explored, especially the energy transfer processes that take place between the PBI fluorophore (donor) and the DAE-CF photochromic unit (acceptor). Energy transfer is too fast to be detected by time-resolved fluorescence (TCSPC), and the measured fluorescence lifetime of the **DAE-PBI** dyad in THF solution is  $6.00 \pm 0.04$  ns before and after irradiation in the UV when the photostationary state at 365 nm is reached, corresponding to the remaining **DAE-PBI** in the OF. Multiscale deactivation processes are recorded when the dyads are gathered into NPs and rationalized their low fluorescence quantum yield, due to the distribution of microenvironments of the PBI fluorophores in the NPs. To estimate the energy transfer rate, femtosecond transient absorption spectroscopy experiments were conducted. The dynamics of the excited state of the dyad at PSS-365 after excitation at 435 nm (PBI is excited through its  $S_0 \rightarrow S_2$  electronic transition) provided us important information concerning the mechanistic scheme in the excited state with interplays between the PBI and DAE-CF units: the PBI in its excited state is at the origin of an ultrafast energy transfer process towards the DAE-CF part, leading to the appearance of a characteristic band of the DAE-CF excited state in 210 fs (in THF solution). Such a time-constant is established as the FRET characteristic time, which is consistent with the expected value at 420 fs derived from the Förster equations. Moreover, the experiments conducted for the **DAE-PBI** dyad in suspension of NPs highlight that efficient FRET processes occur in competition with other deactivation processes in the NPs state. Further detailed studies will be continued in the future to untangle the complex excited state dynamics in NPs.

## Conflicts of interest

On behalf of all authors, the corresponding author states that there is no conflict of interest.

## Acknowledgements

Funding from the Agence Nationale de la Recherche (ANR-17-CE07-0056-01) is acknowledged. CNRS is acknowledged for supporting partially this work through the Nanosynergetics IRP. Chevreul Institute (FR 2638), Ministère de l'Enseignement Supérieur, de la Recherche et de l'Innovation, Hauts-de-France Region and FEDER are acknowledged for supporting and funding partially this work through access to the time-resolved platform.

## References

- (1) Hofmann, M.; Eggeling, C.; Jakobs, S.; Hell, S. W. Breaking the Diffraction Barrier in Fluorescence Microscopy at Low Light Intensities by Using Reversibly Photoswitchable Proteins. *Proceedings of the National Academy of Sciences* **2005**, *102* (49), 17565–17569. <https://doi.org/10.1073/pnas.0506010102>.
- (2) Grotjohann, T.; Testa, I.; Leutenegger, M.; Bock, H.; Urban, N. T.; Lavoie-Cardinal, F.; Willig, K. I.; Eggeling, C.; Jakobs, S.; Hell, S. W. Diffraction-Unlimited All-Optical Imaging and Writing with a Photochromic GFP. *Nature* **2011**, *478* (7368), 204–208. <https://doi.org/10.1038/nature10497>.
- (3) Bates, M.; Huang, B.; Dempsey, G. T.; Zhuang, X. Multicolor Super-Resolution Imaging with Photo-Switchable Fluorescent Probes. *Science* **2007**, *317* (5845), 1749–1753. <https://doi.org/10.1126/science.1146598>.
- (4) Qi, Q.; Li, C.; Liu, X.; Jiang, S.; Xu, Z.; Lee, R.; Zhu, M.; Xu, B.; Tian, W. Solid-State Photoinduced Luminescence Switch for Advanced Anticounterfeiting and Super-Resolution Imaging Applications. *J. Am. Chem. Soc.* **2017**, *139* (45), 16036–16039. <https://doi.org/10.1021/jacs.7b07738>.
- (5) Irie, M.; Fukaminato, T.; Sasaki, T.; Tamai, N.; Kawai, T. A Digital Fluorescent Molecular Photoswitch. *Nature* **2002**, *420* (6917), 759–760. <https://doi.org/10.1038/420759a>.
- (6) Fukaminato, T.; Doi, T.; Tamaoki, N.; Okuno, K.; Ishibashi, Y.; Miyasaka, H.; Irie, M. Single-Molecule Fluorescence Photoswitching of a Diarylethene–Perylenebisimide Dyad: Non-Destructive Fluorescence Readout. *J. Am. Chem. Soc.* **2011**, *133* (13), 4984–4990. <https://doi.org/10.1021/ja110686t>.
- (7) Irie, M.; Fukaminato, T.; Matsuda, K.; Kobatake, S. Photochromism of Diarylethene Molecules and Crystals: Memories, Switches, and Actuators. *Chem. Rev.* **2014**, *114* (24), 12174–12277. <https://doi.org/10.1021/cr500249p>.
- (8) Raymo, F. M.; Tomasulo, M. Electron and Energy Transfer Modulation with Photochromic Switches. *Chem. Soc. Rev.* **2005**, *34* (4), 327. <https://doi.org/10.1039/b400387j>.
- (9) Medintz, I.; Hildebrandt, N. *FRET-Förster Resonance Energy Transfer from theory to application*; Wiley-VCH Verlag GmbH & Co. KGaA, 2014.
- (10) Li, C.; Yan, H.; Zhao, L.-X.; Zhang, G.-F.; Hu, Z.; Huang, Z.-L.; Zhu, M.-Q. A Trident Dithienylethene–Perylenemonoimide Dyad with Super Fluorescence Switching Speed and Ratio. *Nat Commun* **2014**, *5* (1), 5709. <https://doi.org/10.1038/ncomms6709>.

- (11) Fukaminato, T.; Hirose, T.; Doi, T.; Hazama, M.; Matsuda, K.; Irie, M. Molecular Design Strategy toward Diarylethenes That Photoswitch with Visible Light. *J. Am. Chem. Soc.* **2014**, *136* (49), 17145–17154. <https://doi.org/10.1021/ja5090749>.
- (12) Su, J.; Fukaminato, T.; Placial, J.-P.; Onodera, T.; Suzuki, R.; Oikawa, H.; Brosseau, A.; Brisset, F.; Pansu, R.; Nakatani, K.; Métivier, R. Giant Amplification of Photoswitching by a Few Photons in Fluorescent Photochromic Organic Nanoparticles. *Angew. Chem. Int. Ed.* **2016**, *55* (11), 3662–3666. <https://doi.org/10.1002/anie.201510600>.
- (13) Ikariko, I.; Deguchi, S.; Fabre, N.; Ishida, S.; Kim, S.; Kurihara, S.; Métivier, R.; Fukaminato, T. Highly-Stable Red-Emissive Photochromic Nanoparticles Based on a Diarylethene-Perylenebisimide Dyad. *Dyes and Pigments* **2020**, *180*, 108490. <https://doi.org/10.1016/j.dyepig.2020.108490>.
- (14) Ruckebusch, C.; Sliwa, M.; Pernot, P.; de Juan, A.; Tauler, R. Comprehensive Data Analysis of Femtosecond Transient Absorption Spectra: A Review. *Journal of Photochemistry and Photobiology C: Photochemistry Reviews* **2012**, *13* (1), 1–27. <https://doi.org/10.1016/j.jphotochemrev.2011.10.002>.
- (15) Debus, B.; Sliwa, M.; Miyasaka, H.; Abe, J.; Ruckebusch, C. Multivariate Curve Resolution — Alternating Least Squares to Cope with Deviations from Data Bilinearity in Ultrafast Time-Resolved Spectroscopy. *Chemometrics and Intelligent Laboratory Systems* **2013**, *128*, 101–110. <https://doi.org/10.1016/j.chemolab.2013.08.001>.
- (16) Ishibashi, Y.; Nakai, S.; Masuda, K.; Kitagawa, D.; Kobatake, S.; Asahi, T. Nanosecond Laser Photothermal Effect-Triggered Amplification of Photochromic Reaction in Diarylethene Nanoparticles. *Chem. Commun.* **2020**, *56* (1), 7088–7091. <https://doi.org/10.1039/D0CC00884B>.
- (17) Sotome, H.; Nagasaka, T.; Une, K.; Morikawa, S.; Katayama, T.; Kobatake, S.; Irie, M.; Miyasaka, H. Cycloreversion Reaction of a Diarylethene Derivative at Higher Excited States Attained by Two-Color, Two-Photon Femtosecond Pulsed Excitation. *J. Am. Chem. Soc.* **2017**, *139* (47), 17159–17167. <https://doi.org/10.1021/jacs.7b09763>.
- (18) Fron, E.; Schweitzer, G.; Osswald, P.; Würthner, F.; Marsal, P.; Beljonne, D.; Müllen, K.; De Schryver, F. C.; Van der Auweraer, M. Photophysical Study of Bay Substituted Perylenediimides. *Photochem Photobiol Sci* **2008**, *7* (12), 1509–1521. <https://doi.org/10.1039/b813737d>.
- (19) Roozbeh, A.; Bassi, M. de J.; Pereira, A. B.; Roman, L. S.; Buckup, T.; Heisler, I. A. Energy Transfer in Aqueously Dispersed Organic Semiconductor Nanoparticles. *J. Phys. Chem. C* **2020**, *124* (51), 27946–27953. <https://doi.org/10.1021/acs.jpcc.0c09459>.
- (20) Yasukuni, R.; Asahi, T.; Sugiyama, T.; Masuhara, H.; Sliwa, M.; Hofkens, J.; De Schryver, F. C.; Van der Auweraer, M.; Herrmann, A.; Müllen, K. Fabrication of Fluorescent Nanoparticles of Dendronized Perylenediimide by Laser Ablation in Water. *Appl. Phys. A* **2008**, *93* (1), 5–9. <https://doi.org/10.1007/s00339-008-4661-5>.
- (21) Vu, T. T.; Dvorko, M.; Schmidt, E. Y.; Audibert, J.-F.; Retailleau, P.; Trofimov, B. A.; Pansu, R. B.; Clavier, G.; Méallet-Renault, R. Understanding the Spectroscopic Properties and Aggregation Process of a New Emitting Boron Dipyrromethene (BODIPY). *J. Phys. Chem. C* **2013**, *117* (10), 5373–5385. <https://doi.org/10.1021/jp3097555>.
- (22) Dostál, J.; Fennel, F.; Koch, F.; Herbst, S.; Würthner, F.; Brixner, T. Direct Observation of Exciton–Exciton Interactions. *Nat Commun* **2018**, *9* (1), 2466. <https://doi.org/10.1038/s41467-018-04884-4>.
- (23) Ghosh, I.; Ghosh, T.; Bardagi, J. I.; König, B. Reduction of Aryl Halides by Consecutive Visible Light-Induced Electron Transfer Processes. *Science* **2014**, *346* (6210), 725–728. <https://doi.org/10.1126/science.1258232>.
- (24) Kobayashi, Y.; Abe, J. Recent Advances in Low-Power-Threshold Nonlinear Photochromic Materials. *Chem. Soc. Rev.* **2022**, *51* (7), 2397–2415. <https://doi.org/10.1039/D1CS01144H>.
- (25) Nagasaka, T.; Kunishi, T.; Sotome, H.; Koga, M.; Morimoto, M.; Irie, M.; Miyasaka, H. Multiphoton-Gated Cycloreversion Reaction of a Fluorescent Diarylethene Derivative as Revealed by Transient Absorption Spectroscopy. *Phys. Chem. Chem. Phys.* **2018**, *20* (30), 19776–19783. <https://doi.org/10.1039/C8CP01467A>.